JET PUMP RISER WELD FLAW EVALUATION HANDBOOK FOR HATCH UNIT 1

December 1997

Prepared by: Asherlekar
Aroon Herlekar, Principal Engineer
Structural Mechanics & Materials

Verified by:
Hardayal Mehta, Technical Leader
Structural Mechanics & Materials

Reviewed by: T A Caine 12/18/97
Tom A. Caine, Manager
Structural Mechanics & Materials

IMPORTANT NOTICE REGARDING CONTENTS OF THIS REPORT

Please Read Carefully

The only undertakings of the General Electric Company (GE) respecting information in this document are contained in the contract between Southern Nuclear Operating Company (SNC) and GE, and nothing contained in this document shall be construcd as changing the contract. The use of this information by anyone other than SNC, or for any purpose other than that for which it is intended, is not authorized; and with respect to any unauthorized use, GE makes no representation or warranty, express or implied, and assumes no liability as to the completeness, accuracy, or usefulness of information contained in this document, or that its use may infringe privately owned rights.

Executive Summary

A flaw evaluation, consisting of stress and fracture mechanics analyses of the Hatch Unit 1 jet pump circumferential riser welds was conducted to develop a flaw evaluation handbook. The procedures of BWRVIP-41, were used as a guide in determining the allowable flaw lengths. End-of-cycle allowable flaw lengths were calculated at three circumferential weld locations. The methodology presented in this report can be used along with consideration of observed IGSCC, and evaluation of fatigue crack growth rates to disposition any indications detected during future inspections of the jet pumps at Hatch Unit 1.

The following table shows a summary of allowable adjusted flaw lengths for Hatch 1.

Allowabl Adjusted Circumferential Flaw Sizes

Weld	Flaw Length (inch)
RS-1	15.42
RS-2	16.69
RS-3	19.87

Observed indications less than 5.8" in length, after consideration of IGSCC growth and NDE uncertainty, do not have to be further evaluated.

TABLE OF CONTENTS

	Page
1. PURPOSE/OBJECTIVE	5
2. METHODS	5
3. ASSUMPTIONS	6
4. DESIGN INPUTS	7
4.1. Applied Loads	7
5. LOAD COMBINATIONS AND STRESS LEVELS	12
5.1. Load Combinations	12
5.2. Calculated Stress Levels	13
6. FRACTURE MECHANICS EVALUATION	14
6.1. Limit Load Methodology	14
6.2. Allowable Flaw Length Calculation	16
6.3. Crack Growth Evaluation	16
6.4. Procedure for Evaluation of Indications using Handbook	17
7. LEAKAGE CALCULATION	18
8. SUMMARY AND CONCLUSIONS	19
9. REFERENCES	20

1. PURPOSE/OBJECTIVE

The objective of this report is to document the results of a fracture mechanics evaluation of the Hatch Unit 1 jet pump riser pipe circumferential welds. This evaluation results in the allowable end-of-cycle flaw lengths at the three riser pipe circumferential welds designated as welds RS-1, RS-2, and RS-3 per BWRVIP-41 (Reference 1) and are shown in Figure 1.

The results presented in the flaw evaluation handbook can be used to disposition indications found in the jet pump riser pipes at Hatch Unit 1.

2. METHODS

This section presents the methodology and procedure used in performing the jet pump riser pipe weld flaw evaluation. Following are the steps used in the analysis.

1. Review of the reference drawings.

2. Determine the loading and load combinations as suggested in BWRVIP-41 (Reference 1). In addition, the changes to the loads due to extended power uprate (EPU) at Hatch 1 are also incorporated in the loads and load combinations considered.

3. Create a SAP4G07V (Reference 2) finite element model for the jet pump. Anchor connection points are the recirculation inlet nozzle, shroud support plate and riser brace.

4. Determine the membrane and bending stresses considering the load combinations.

5. Use the limit load methods of BWRVIP-41 as a guide to determine the allowable flaw lengths. BWRVIP-41 evaluation procedures are used as a guide, since the jet pump is not a part of the reactor pressure boundary.

6. Evaluate IGSCC and fatigue crack growth rate. Calculate IGSCC crack growth for eighteen months (12,000 hrs) cycle based on a growth rate of $5x10^{-5}$ inch/hot hour. Determine if fatigue crack growth rate due to vibration is significant by calculating the

stress intensity factor due to flow induced vibration and comparing with threshold stress intensity. If actual stress intensity is less than threshold, than given crack is acceptable.

7. Leakage curves are calculated which show leakage versus percent of allowable flaw during normal plant operation per BWRVIP-41.

3. ASSUMPTIONS

1. The jet pump geometry is as described in the reference drawings (Reference 5). The dimensional tolerances specified on the reference drawings are such that any variations within those values will have insignificant impact on the calculated stress values. It was also judged that any deviations between the as-built geometry and the geometry indicated in the reference drawings would not be significant in terms of stress analysis and the allowable flaw calculations.

2. The calculations are based on one flaw per riser. However, synergistic effects of multiple flaws in one riser are negligible and would not affect the results of this analysis. The reason is that even large flaws (180 degrees) do not significantly change the stiffness of the riser and therefore the response to input loading does not change.

3. Fatigue due to thermal stresses is negligible due to minimal temperature differentials during normal or transient conditions.

4. The jet pumps are assumed to be in the as-designed configuration because the vibration data on which the fatigue evaluation is based was taken from a new plant in startup. Issues such as jet pump fouling and restrainer bracket set screw gap may affect this assumption in a non-conservative manner. Even though all jet pumps have not yet been inspected, the review of the results of 6 out of 10 previously inspected and 2 out of 10 inspected during 1997 outage jet pump pairs inspection data demonstrates that there is no history of set screw gaps or degradation at Hatch 1. Ten out of 10 Hatch 2 jet pump pairs have been previously inspected to confirm that set screw tack welds are intact. Six out of 10 Hatch 2 jet pump pairs have been previously inspected to confirm that there are no set screw or restrainer wedge gaps. However, in the vibration fatigue evaluation other conservative aspects of analysis more than adequately compensate for potential nonconservatism here.

4. DESIGN INPUTS

The design inputs in this evaluation consisted of the geometry of the jet pump and the applied loads. The geometry of the jet pump was obtained from the drawings listed in Reference 5.

The jet pump riser pipe is 10-inch schedule 30 while the thermal sleeve is 10-inch schedule 40 and the material for both is Type 304 stainless steel (Reference 5). Figure 1 shows a schematic of the jet pump. The welds in Figure 1 have been designated as RS-1 through RS-3 in accordance with BWRVIP-41 designations. A finite element model was developed to determine the stresses from various design loads. Figure 2 shows a line plot of the finite element model. The SAP4G07V finite element program was used to perform the stress analysis.

4.1. Applied Loads

The applied loads on the jet pump assembly consist of the following: deadweight, seismic inertia, seismic anchor displacements, hydraulic, fluid drag, loads due to flow induced vibrations, and thermal anchor displacements. Each of these loads are briefly discussed in the following sections.

4.1.1. DeadWeight (DW)

The deadweight loading consists of the weight of the jet pump and the entrapped water. The stresses for this loading were calculated by applying one 'g' vertical acceleration in the finite element model of the jet pump assembly. For flaw evaluation purposes, the stress from this loading is treated as primary.

4.1.2. Hydraulic Loads (F1, F2)

The hydraulic loads acting on the jet pump are calculated by summing the fluid momentum and pressure forces in the vertical and horizontal directions. This load definition considers any pressure differences between the annulus and the jet pump. Two hydraulic force values are calculated and applied to the jet pump. The first value is the horizontal force in the riser pipe which puts the riser elbow to sleeve weld in tension. The second value is the net vertical hydraulic load. The net vertical force is predominately caused by the pressure difference between the diffuser and inlet-mixer slip joint. Because the slip joint can not transmit a vertical load, the vertical load is carried through the riser pipe causing a bending moment on the riser. The following designations are used:

Normal Horizontal and Vertical Hydraulic Load: F1
Faulted Horizontal and Vertical Hydraulic Load: F2

For the flaw evaluation purposes, the stresses from the hydraulic loads are treated as primary. The values of the hydraulic loads are given in the table below.

Hydraulic Loads

Designation	Horizontal Load (lb)	Vertical Load(lb)
F1	16,940	9,521
F2	16,940	11,276

Since the F2 load in the vertical direction is slightly higher than the F1 vertical load but the dominant horizontal load is same in both conditions, F2 loads are conservatively used in all load combinations.

4.1.3. Seismic Inertia

The seismic inertia loading consists of horizontal and vertical inertia forces acting on the jet pump due to seismic excitation of the RPV (Reference 6). The seismic excitations are as a result of the core shroud repair program reanalysis of the Hatch 1 primary structural model. The locations where the seismic excitation is imparted to the jet pump are the vessel recirculation inlet nozzle, the shroud support plate and the riser brace. During seismic inertial loading analysis, mass of jet pump, water entrapped in it, and the hydrodynamic masses were considered. The following designations are used:

Operating Basis Earthquake Inertia: OBEI
Safe Shutdown (Design Basis) Earthquake Inertia: SSEI

The natural frequency of the jet pump is high (>20 Hz) such that the horizontal acceleration values from the response spectra (envelop at RPV nodes 41 and 49) at 20 Hz are used in a static "g" analysis. The vertical ZPA (accelerations) values were taken as 2/3 of the peak ground accelerations of 0.08 g (OBE) and 0.15 g (DBE). The acceleration values are multiplied by a conservative factor of 1.5 to account for higher modes effects. The values used in the evaluation are shown in the following table. The net seismic forces and moments are taken as maximum of X+Y or X+Z, where X, Y, and Z are three separate static acceleration cases analyzed using the values shown below.

Seismic Accelerations

	Horizontal (Y and Z)	Vertical (X)
OBEI	0.45	0.08
SSEI	0.60	0.15

NOTE: Hatch 1 has a special seismic evaluation requirement called "1/2 SME" Time History Evaluation. This is an alternate to the DBE loading. The acceleration values for DBE shown above are envelope of DBE or 1/2 SME. Thus no separate loading condition and combinations incorporating 1/2 SME are documented further in this handbook.

For the purposes of flaw evaluation, the stresses from the seismic inertia loads are treated as primary.

4.1.4.Seismic Anchor Displacements

The seismic anchor displacement loading consists of relative horizontal and vertical displacements between the shroud support plate, recirc inlet nozzle and riser brace attachment points to the RPV. Due to relatively short elevation difference between these points and RPV itself having small displacements, relative horizontal displacements (Reference 6) have insignificant effect on flaw evaluation results, and therefore, are taken as zero. Similarly, RPV being rigid in the vertical direction, there are no relative vertical seismic anchor movements between recirc inlet nozzle and the riser brace attachment points to the RPV. The relative displacements are negligible for both OBE and DBE loading.

Operating Basis Earthquake Displacements:	OBED
Safe Shutdown Earthquake Displacements:	SSED

For the purposes of flaw evaluation, the stresses from the seismic anchor displacements loads are treated as secondary.

4.1.5. Fluid Drag and Acoustic Loads

The drag loads consist of the forces resulting from the fluid flowing in the annulus region past the jet pump. The flow in the annulus region during normal operation exerts some downward drag force on the jet pump. The magnitude of the stress from this loading is less than 5% of drag load due to LOCA and even less 5% of that from the weight loading. This is because the flow velocity during normal condition is only 23% of that during LOCA and the drag load is proportional to velocity square term and is therefore, neglected in the Normal/Upset load combinations. A postulated recirculation line break LOCA (suction side) subjects the jet pump to a drag force load in a tangential direction relative to vessel centerline. A previous TRACG analysis (Reference 7) performed for a similar size plant calculated the worst case flow velocities past the jet pump assembly. These velocities were adjusted upw lly for Hatch 1 unique geometry. The worst case velocities correspond to a suction side recirculation line break LOCA. Other breaks do not affect the jet pump nearly as severely due to the other lines proximity or size. The velocities, used in the calculation of the drag forces, correspond to the jet pumps nearest to the suction nozzle. The horizontal drag loads on the jet pump were determined to be approximately 900 lb on the riser and 2310 lb on the diffuser. The following designation is used:

Drag Loads During Normal Operation:	DRG1
Drag Loads During LOCA Condition:	DRG2

The LOCA drag load consists of the acoustic component (FAC) and the flow induced drag (DRG2) component. The acoustic component (FAC) of load is a momentary shock load and the flow induced drag component (DRG2) of load follows acoustic load in time. Therefore, the time phasing of the two components of this load are considered during Faulted load combination.

For the purposes of flaw evaluation, the stresses from the circumferential drag loads are treated as primary and the radial drag (due to vortex shedding) loads are negligible due to their low frequency (jet pump fundamental frequency being more than 3 times greater than vortex shedding frequency, thus requiring no evaluation).

4.1.6. Flow Induced Vibration (FIV)

The flow induced vibration (FIV) loads are caused by turbulent flow in the piping exciting the natural frequencies of the jet pump assembly. The method of calculating the vibration stress from the test data is summarized below.

1. Review the startup vibration data (Reference 8) to determine the primary modes of interest for the jet pump

2. Using a finite element model of the jet pump, determine the natural frequencies, mode shapes, and modal stresses of all modes of interest.
3. Normalize the modal stresses such that the they are equal to the measured data observed during startup testing.
4. Select the highest normalized modal stress at the weld location on the riser pipe from all modes. This is the FIV stress; 1150 psig peak to peak with R ratio = 0.25, bounds all three weld locations.

For Hatch 1, modal extraction analysis was performed. Because the same vibration startup data for Fitzpatrick, prototype of BWR/4 218 plant (Reference 9), is applicable for Hatch 1, the FIV stresses calculated for Fitzpatrick are applicable.

For the purposes of flaw evaluation, the FIV stresses are treated as primary.

4.1.7. Thermal Anchor Displacements

The three anchor points of the jet pump (the recirculation inlet nozzle, riser braces on the vessel, and the shroud support plate) grow vertically and horizontally at different rates due to differences in the materials (low alloy steel for the vessel, versus stainless steel for the jet pump). The loads produced by the thermal anchor displacements are treated as secondary for the purposes of the flaw evaluation. The following thermal displacements are considered:

Displacements during Normal Operation:	NOD
Displacements during Loss of Feed Water Pump Transient:	LWFPD
Displacements during LOCA thermal effects:	LOCAD

The displacements are calculated at normal operating (NOD) temperature which is 552°F (including extended power uprate) for region B according to the reactor thermal cycle diagram and power uprate design specification (Reference 9). The displacement effects for LFWPD case are about the same as NOD case but are of non controlling nature since the transient temperature is 300^0F in the jet pump while RPV is still at 552°F (with very low pressures) and thus this case is considered enveloped by NOD case in all load combinations. The LOCAD case displacements are also enveloped by NOD case since the RPV temperature (approximately equal to the drywell temperature) is 290^0 F per UFSAR Figure 5.2-21 (sheets 3 and 5 of 5) which is lower than NOD case and thus this case is also not considered in any load combinations. The RPV pressure dialation effects in the radial direction (displacements of RPV due to pressures) are same at the recirculation inlet nozzle and the riser brace attachment locations to the RPV for any one of the above described events. RPV pressure dialation effects in the vertical direction are considered insignificant in flaw size calculations and therefore, are taken as zero. Thus their relative values are zero and thus the pressure dialation effects of RPV is neglected. Incidentally, the hydraulic loads already include the pressure differential across the riser pipe.

5. LOAD COMBINATIONS AND STRESS LEVELS

This section describes the manner in which the various loads were combined for the purpose of obtaining stress levels for the flaw evaluation. The limiting stress levels at the welds are then summarized.

5.1. Load Combinations

The flaw evaluation methodology to be used makes the distinction between primary and secondary stresses by specifying different safety factors. The flaw evaluation methodology also makes the distinction between the normal/upset (Level A/B) condition loads, for which the factor of safety is 2.77, and the emergency/faulted (Level C/D) condition loads, for which the safety factor is 1.39. The load combinations are consistent with Hatch 1 UFSAR.

The following set of the controlling load combinations were considered for the evaluation of normal/upset condition:

(1) DW(P) +F1(P) + FIV(P) + NOD(S)

(2) DW(P) +F1(P) + FIV(P) + OBEI(P) + NOD(S)

The set of the controlling load combinations used for the Emergency/Faulted conditions are the following:

(3) DW(P) + F2(P) + SSEI(P) + NOD(S)

(4) DW(P) + F2(P) + SSEI(P) + DRG2(P) + NOD(S)

(4ALT) DW(P) + F2(P) + SSEI(P) + FAC(P)(P) + NOD(S)

Note that the letter 'P' or 'S' in the parenthesis indicates whether a load is primary or secondary as defined by the ASME Code. When the acoustic load component (FAC) of

LOCA load is included along with F2(P) load in load combination (4ALT), the DRG2(P) load is deleted from the load combination (4ALT) to account for the time phasing of the drag and acoustic portions of the LOCA load.

5.2. *Calculated Stress Levels*

The forces and moments at various nodes in the model for all of the load sources were calculated using the SAP4G07V finite element code (Reference 2). These forces and moments were then combined to obtain the total forces and moments for a given load combination. Thus, for each load combination and each node, a set of forces and moments were obtained. Furthermore, within each set, the forces and moments from the displacement-controlled loading were tabulated separately for the calculation of expansion stress. As described later, the flaw evaluation methodology uses the primary membrane (P_m), primary bending (P_b) and the expansion stress (P_e).

The calculated values of P_m, P_b and P_e stress levels at the circumferential weld locations are summarized in the following tables for the governing load combinations for Normal/Upset and Emergency/Faulted service levels. Major contribution (more than 80%) to these stresses is from hydraulic load.

Calculated Stress in Governing Normal/Upset Load Combinations

Weld ID (Figure 1)	P_m (psi)	P_b (psi)	P_e (psi)	Load Combination
RS-1	1795	2184	413	2
RS-2	945	2424	222	2
RS-3	1025	801	102	2

Calculated Stress in Governing Emergency/Faulted Load Combinations

Weld ID (Figure 1)	P_m (psi)	P_b (psi)	P_e (psi)	Load Combination
RS-1	3221	1652	413	4ALT
RS-2	951	1877	222	4
RS-3	1029	291	102	4

The stress levels in the preceding tables were used in the allowable flaw evaluations as described in the next section.

6. FRACTURE MECHANICS EVALUATION

The limit load methodology was used in calculating the allowable flaw lengths. This methodology is first described followed by the results of allowable flaw evaluations.

6.1. Limit Load Methodology

Consider a circumferential crack of length, $l = 2R\alpha$ and constant depth, d. In order to determine the point at which limit load is achieved, it is necessary to apply the equations of equilibrium assuming that the cracked section behaves like a hinge. For this condition, the assumed stress state at the cracked section is as shown in Figure 3 where the maximum stress is the flow stress of the material, σ_f. Equilibrium of longitudinal forces and moments about the neutral axis gives the following equations:

$$\beta = [(\pi - \alpha d/t) - (P_m/\sigma_f)\,\pi]/2 \qquad (1)$$

$$P_b' = (2\sigma_f/\pi)\,(2 \sin\beta - d/t \sin\alpha) \qquad (2)$$

Where,

- t = pipe thickness
- α = crack half-angle as shown in Figure 3
- d = crack depth
- R = pipe mean radius
- β = angle that defines the location of the neutral axis
- Z = weld type factor
- P_e = piping expansion stress
- P_m = primary membrane stress
- P_b = primary bending stress
- P_b' = failure bending stress
- $\sigma_f = 3S_m$ flow stress
- S_m = allowable stress

The safety factor (SF) is then incorporated as follows:

$$P_b' = Z{*}SF\,(P_m + P_b + P_e/SF) - P_m \qquad (3)$$

The P_m and P_b are primary stresses. P_e is a secondary stress and includes stresses from all displacement-controlled loadings such as thermal expansion, seismic anchor motion, etc. All three quantities are calculated from the analysis of applied loading. The safety factor value is 2.77 for normal/upset conditions and 1.39 for emergency/faulted conditions. The crack angle (2α) is the value for which equation 2 is equal to equation 3.

Z Factor

The test data considered by the ASME Code indicated that the welds produced by a process without using a flux had fracture toughness as good or better than the base metal. However, the welds produced by a process using flux had lower toughness. To account for the reduced toughness of the flux welds (as compared to non-flux welds) the Section XI procedures prescribe a penalty factor, called a 'Z' factor. The examples of flux welds are submerged arc welds (SAW) and shielded metal arc welds (SMAW). Gas metal-arc welds (GMAW) and gas tungsten-arc welds (GTAW) are examples of non-flux welds. Figure IWB-3641-1 may be used to define weld-base metal interface. The expressions for the value of Z factor in Appendix C are given as the following:

$$Z = 1.15\,[1 + 0.013(OD-4)] \text{ for SMAW}$$
$$= 1.30\,[1 + 0.010(OD-4)] \text{ for SAW}$$

where OD is the nominal pipe size (NPS) in inches. The procedures of Appendix C recommend the use of OD = 24 for pipe sizes less than 24-inches. This approach is very conservative and, therefore, the use of actual NPS (OD = 10 inches) was made in calculating the 'Z' factor. This approach is considered reasonable as recent discussions in the Section XI Code Working Group on Pipe Flaw Evaluation indicate that for small diameter pipes, such as the 10-inch diameter jet pump riser pipe, the Z-factor may be close to or less than 1.0. The welding process used was a combination of shielded metal arc type (SMAW) or submerged arc welds (SAW) and gas tungsten arc weld type (GTAW). Since a non-flux process (GTAW) was specified for only part of the weld, it must be assumed that the welds are flux welds (SAW). The Z-factor is thus:

$$Z_{10\text{-inch}} = 1.30\,[1 + 0.013(10-4)] = 1.38$$

6.2. Allowable Flaw Length Calculation

The stresses from the table in the preceding section were utilized to determine the acceptable through-wall flaw lengths. The acceptable flaw size was determined by requiring a safety factor on stress. The flow stress was taken as $3S_m$ (S_m = 16.9 ksi for Type 304 stainless steel at 550°F). As specified in Reference 3, safety factors of 2.77 for the normal/upset conditions and 1.39 for the emergency/faulted conditions, respectively, were used. The calculated values of the end-of-cycle allowable flaw lengths are tabulated in the following table. These allowable flaw lengths conservatively assume all welds are flux welds (SAW).

Maximum Allowable Flaw Lengths Based on Outside Diameter

Weld	Flaw Length (inch)
RS-1	15.42
RS-2	16.69
RS-3	19.87

These allowable values are the end of cycle values and they do not consider the crack growth due to IGSCC, fatigue, or NDE uncertainty. The crack growth is discussed in Section 6.3.

6.3. Crack Growth Evaluation

Prior crack growth analyses performed for BWR shroud and core spray line indications have used a IGSCC crack growth rate of $5x10^{-5}$ inch/hot hour. This crack growth rate translates into a crack length increase per eighteen months cycle of approximately (12,000 hrs x $5x10^{-5}$) or 0.60 inch at each end of an indication. Thus, the projected length, l_f of any indication whose current length at the time of inspection is, l_p, would be (l_p + 0.60 x 2) inches. A factor of 2 in the preceding parenthesis is to account for the growth at each end of the indication.

In addition to IGSCC growth, fatigue growth due to flow induced vibration (FIV) is discussed. The expected fatigue growth is a strong function of the crack size and orientation and cannot be determined until an indication is characterized. With a characterized crack, the stress intensity factor (ΔK) can be computed and compared to the threshold stress intensity factor (ΔK_{th}). The ΔK_{th} is the value at which fatigue crack growth for high cycle stress becomes significant for high cycle events and must be considered. At values below ΔK_{th}, fatigue growth is zero. For 304 stainless steel, Reference 10 reports a ΔK_{th} value of approximately 5.5 ksi$\sqrt{in}$ at R ratio of <0.5. A threshold value of 5.0 ksi$\sqrt{in}$ is used here to cover vibration loading uncertainties. For peak alternating stress intensity of 1150 psi, with

R < 0.5, the 5 ksi is conservative since ΔK is directly proportional to stress intensity, lower amplitude of R will give lower fatigue allowable crack size. The allowable crack size due to FIV was based on the stress intensity calculation method described in Reference 11. The smallest calculated EOC crack size for the three locations is 5.8 inches. This value is less than the limit load method allowables, therefore, fatigue crack growth would begin prior to reaching the limit load crack length.

Thermal expansions were also considered in evaluating fatigue. However, the fatigue crack growth due to thermal expansion stress cycling is negligible due to the limited number of cycles and low thermal stress intensities. The loading cycles are primarily the heatup/cooldown events. Total crack growth for thermal transients is insignificant.

6.4. Procedure for Evaluation of Indications using Handbook

Any indications at HAZ of the welds 1, 2 and 3 (Figure 1) can be evaluated by use of this handbook as follows.

With a crack growth of 0.6 inch at each end of the both indications, total actual flaw size at the End-Of -Cycle including NDE uncertainty values of '2t' (Reference 12) are as shown in the Table below.

Flaw Sizes After one Cycle

Indication Location Weld	Indication Measured Length	IGSCC Growth*	NDE uncertainty (2t)	Adjusted Size (Inches)	Allowable Flaw Size (Limit Load)	Allowable Flaw Size (FIV)
RS-1	2A"	1.2"	0.61"	2A + 1.81	15.42"	5.8"
RS-2	2B"	1.2"	0.61"	2B + 1.81	16.69"	5.8"
RS-3	2C"	1.2"	0.61"	2C + 1.81	19.87"	5.8"

(*) Since Hatch 1 has installed Hydrogen Water Chemistry IGSCC mitigation measures, the calculated IGSCC crack growth of 1.2 inches is very conservatively.

If the adjusted flaw lengths after one cycle are less than the allowable flaw sizes, then the existing flaws are acceptable for continued operation without any modifications.

7. LEAKAGE CALCULATION

Leakage from postulated through-wall flaws with length equal to the allowable end of cycle (EOC) flaw size are calculated in this section. The leakage rate through an indication was estimated assuming incompressible Bernoulli flow:

$$Q = CA\sqrt{2g_c \Delta P / \rho} \qquad (5)$$

where, Q = Leakage

C = flow coefficient

A = area

ρ = mass density of fluid

ΔP = pressure difference across the pipe/vent

A riser ΔP value of 173 psid is used which bounds the jet pump normal flow conditions for the plant. This is the design value for the steady state pressure difference during the jet pump operation for Hatch 1.

Leak rate from the through-wall indications in the riser pipe can be estimated using the preceding equation with the value of flow coefficient, C, assumed as 1.0. A key input needed is the crack opening area, A.

The approach used in this evaluation to calculate the value of A, was to calculate a conservative value of crack opening displacement, δ, and assume the crack opening configuration to be like a rectangular slot with one side being the crack length, 2a, and the other side as the crack opening displacement. The conservative crack opening was assumed as 10 mils. The crack opening area is then simply:

$$A = 2a\,(\delta) \qquad (6)$$

Figure 4 shows leakage rates versus the percentage of the allowable flaw size calculated in Section 8.0.

The leakage through the allowable flaw lengths is insignificant compared to the drive flow during normal operation and compared to LPCI flow during accident scenarios, so the allowable flaw sizes are acceptable from a leakage perspective.

8. SUMMARY AND CONCLUSIONS

A flaw evaluation, consisting of stress and fracture mechanics analyses of the Hatch Unit 1 jet pump circumferential riser welds was conducted to develop a flaw evaluation handbook. The procedures of BWRVIP-41, were used as a guide in determining the allowable flaw lengths. End-of-cycle allowable flaw lengths were calculated at three circumferential weld locations. The methodology presented in this report can be used along with consideration of observed IGSCC, and evaluation of fatigue crack growth rates to disposition any indications detected during future inspections of the jet pumps at Hatch Unit 1.

The following table shows a summary of allowable adjusted flaw lengths for Hatch 1.

Allowable Adjusted Circumferential Flaw Sizes

Weld	Flaw Length (inch)
RS-1	15.42
RS-2	16.69
RS-3	19.87

Observed indications less than 5.8" in length, after consideration of IGSCC growth and NDE uncertainty, do not have to be further evaluated. However, for indications greater than 5.8" in length, after IGSCC growth and NDE uncertainty, fatigue crack growth is predicted prior to the allowable flaw length shown in the above table.

9. REFERENCES

[1] BWR Jet Pump Assembly Inspection and Flaw Evaluation Guidelines, (BWRVIP-41), EPRI Report No. TR-108728, October 1997.

[2] SAP4G07V Users Manual, NEDO 10909, Addenda 1, Revision 1, 1996.

[3] ASME Boiler and Pressure Vessel Code, Section XI, Rules for In-Service Inspection of Nuclear Power Plant Components, American Society of Mechanical Engineers, 1989 Edition, Paragraph IWB 3640.

[4] Ranganath, S. and Mehta, H. S., "Engineering Methods for the Assessment of Ductile Fracture Margin in Nuclear Power Plant Piping," Elastic-Plastic Fracture: Second Symposium, Volume II - Fracture Resistance Curves and Engineering Applications, ASTM STP 803, C.F. Shih and J. P. Gudas, Eds., American Society for Testing and Materials, 1983, pp. II-309 - II-330.

[5] Hatch Unit 1 Jet Pump Drawing No. 729E647
Hatch Unit 1 Jet Pump Riser Drawing No. 117C2809
Hatch Unit 1 Jet Pump Elbow Drawing No. 117C3250
Hatch Unit 1 Reactor Vessel Drawing No. 920D841BB
Hatch Unit 1 Riser Brace Drawing No. 117C4353 and 4354.
Hatch Unit 1 Reactor Drawing No. 197R589

[6] Hatch Unit 1 Seismic Analysis, as follows;

a GENE Letter from S. H. Pang to C. V. Syx (SNOC) "In structure response spectra for DBE and OBE at different nozzle elevations affected by the Modified Core Shroud for Hatch Unit 1" dated October 5, 1994.

b GENE -771-48-0894, Rev. 1, "Seismic Design Report of the Shroud for Hatch 1", dated September 21, 1994.

c GENE-771-48-0894, dated September 21, 1994, "Hatch 1 Shroud Repair 1 /2 SME Time History Seismic Analysis".

d GE letter to Brad Harkins from Michael P. Schrag, dated January 24, 1995, " Transmittal of various response spectra for Hatch 1".

[7] DRF # A71-00014, Index C-13, TRACG Acoustic Loads Analysis and DRF # A13-402, Vol. X, Index 3.2, 3.3, Hatch 1 & 2 EPU changes.

[8] Fitzpatrick Vibration Measurements- Final report, NEDE-23673, Class III, August 1977.

[9] Hatch Unit 1 Reactor Thermal Cycles Drawing No. 729E762, Nozzle Thermal Cycles Drawing No. 135B9990, and Power Uprate Specification 25A5541.

[10] Barsom, J. M., Rolfe, S. T., Fracture and Fatigue Control in Structures, Second Edition, Prentice-Hall, Inc.

[11] Zahoor, A., Ductile Fracture Handbook, Prepared for Novetech Corporation and EPRI, EPRI Report Number NP-6301-D.

[12] BWR Vessel and Internals Project, Reactor Pressure Vessel and Internals Examination Guideline (BWRVIP-03), EPRI Report TR-105696, October 1995.

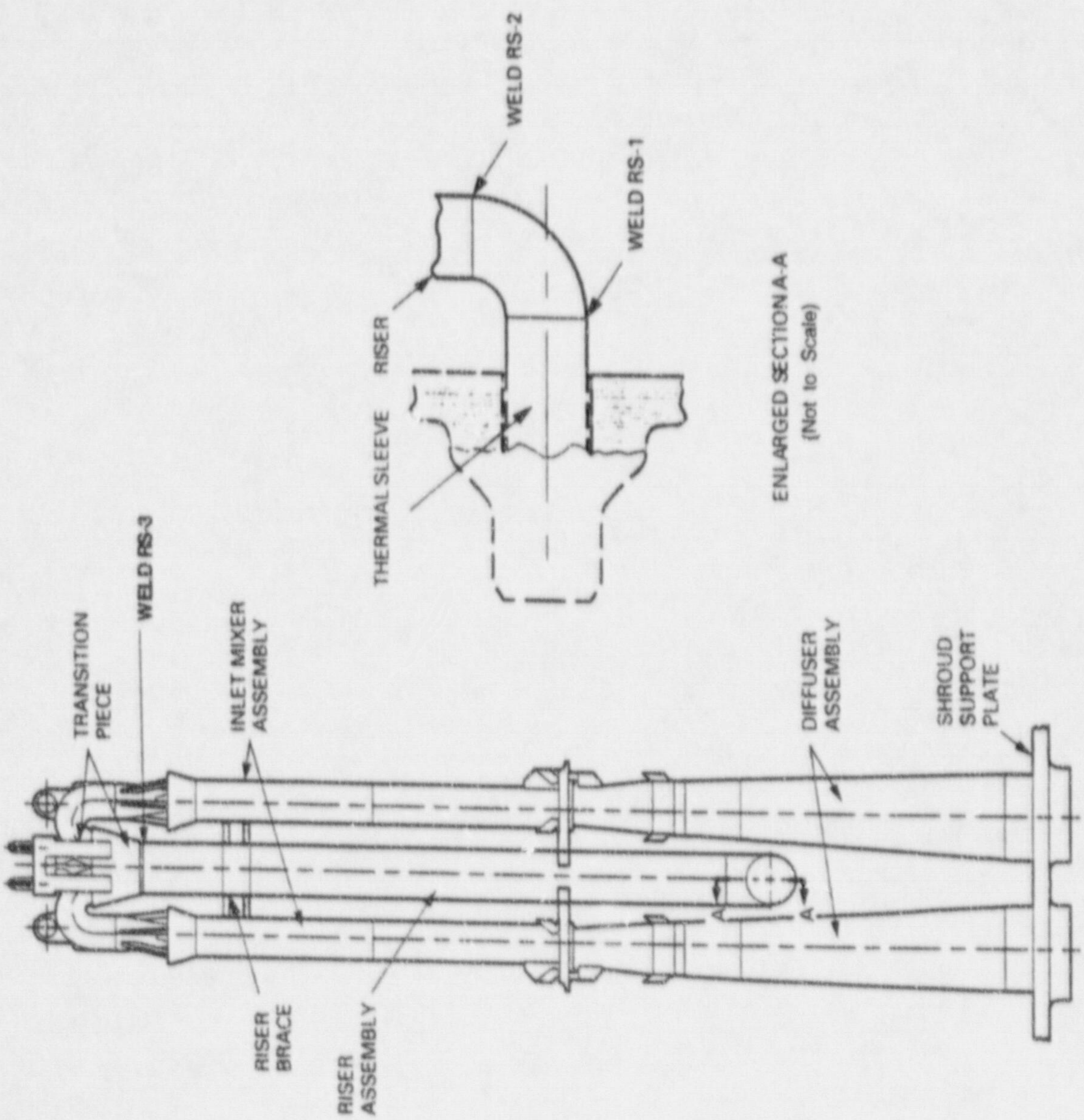

Figure 1. Weld Locations on Hatch Unit 1 Jet Pump

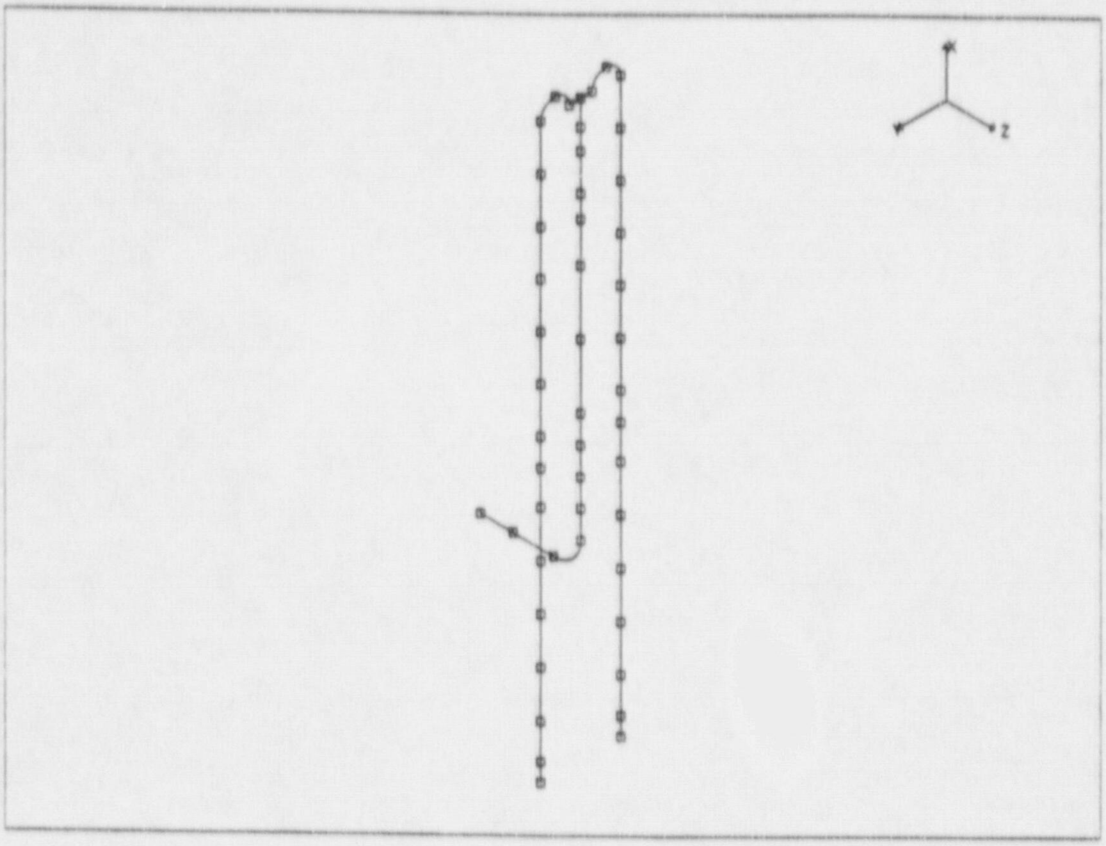

Figure 2. SAP Model of the Hatch Unit 1 Jet Pump

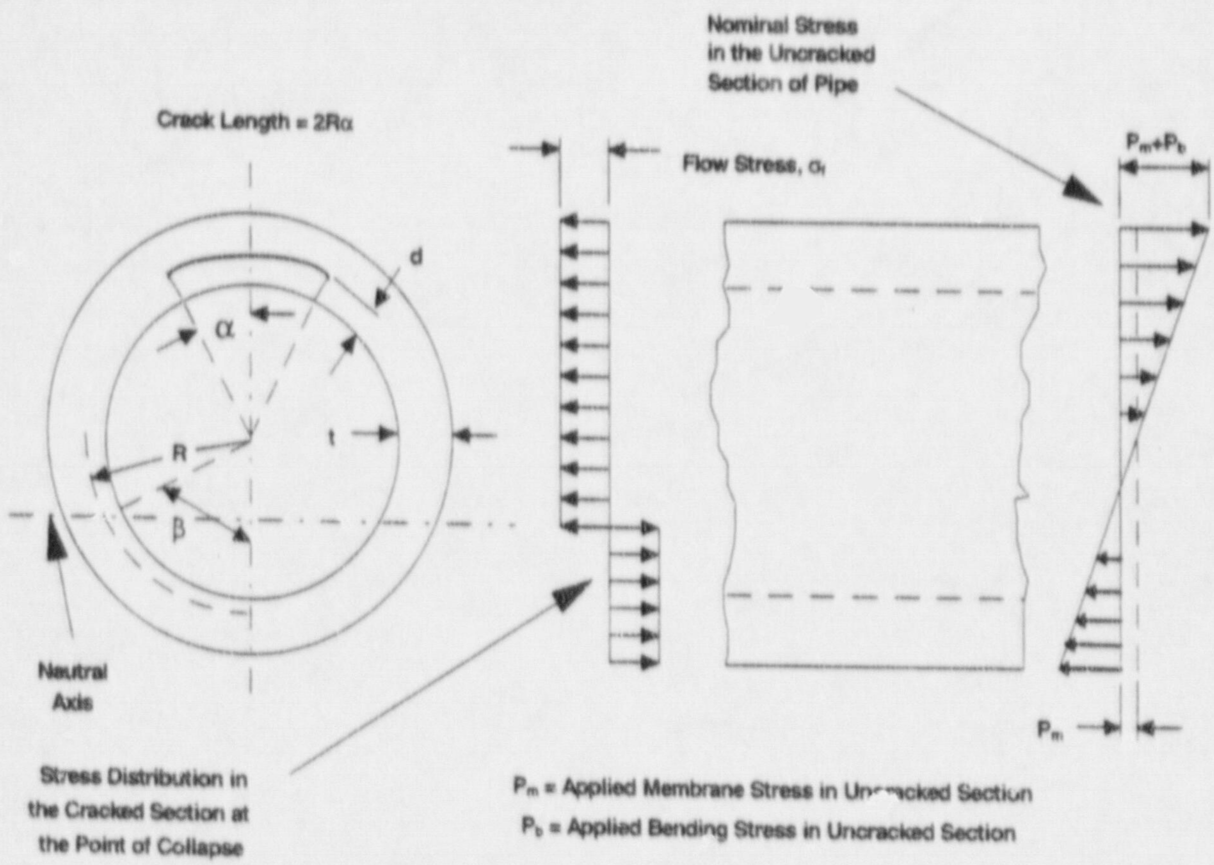

Figure 3. Stress Distribution in a Cracked Pipe at the Point of Collapse

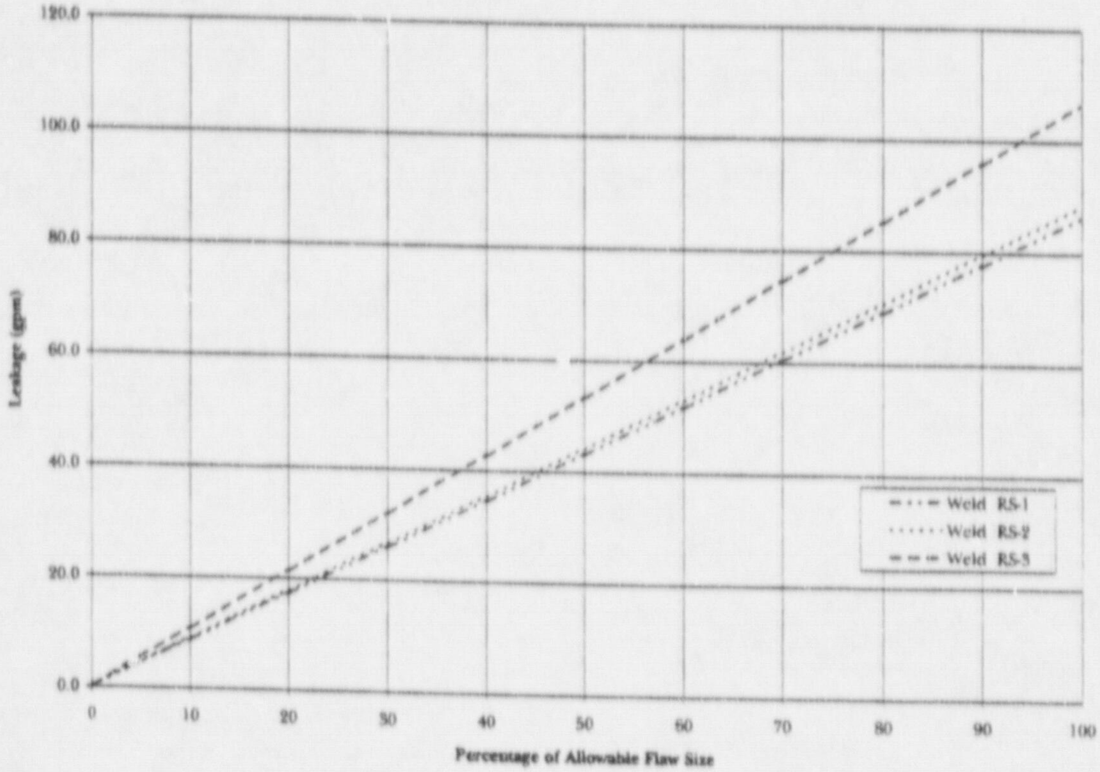

Figure 4. Leakage Versus Percentage of Allowable Flaw Size

Attachment 2

Evaluation of Indications in the Unit 1 Shroud Core Plate Support Ring (GENE-523-B1301869-12L1)

GE Nuclear Energy

General Electric Company
175 Curtner Avenue, San Jose, CA 95125

GENE-523-B1301869-122L1

October 31, 1997

Mr. Denver Atwood
Southern Nuclear Co.
40 Inverness Parkway
Birmingham, AL 35242

cc: K Faynshtein, GE
W Grimme, GE
L Patterson, GE
DRF B13-01869-122

Subject: **Evaluation of Indication in the Unit 1 Shroud Core Plate Support Ring**

References: [1] Indication Notification I97H1002.

Dear Denver,

This letter presents the results of our technical evaluation of an indication [1] in the Unit 1 core plate support ring segment weld at 180° (see Figure 1). In summary, the existing 0.3 inch long indication could grow assuming bounding IGSCC rates to 0.9 inches during the upcoming 18 month operating cycle. This is smaller than our conservatively estimated allowable flaw length of 3.6 inches, so the integrity of the ring is well within acceptable limits for at least one cycle of operation.

Approach

The following steps and associated assumptions were used in the analysis:

1. The 0.3 inch indication, as shown in Figure 1, was assumed to exist radially across the entire 6.5 inch depth of the ring. This extends the crack several inches beyond the H6B weld heat affected zone where a crack could be postulated to initiate, and is therefore a conservative flaw consideration.

2. The normal operation and LOCA delta-P loadings on the ring have been multiplied by a conservative factor of 5. This conservatism eliminates the need to consider detailed loading or load combinations and covers higher delta-P values that would apply with extended power uprate.

3. The loading assumption on the ring takes no credit for the load carried by the core plate holddown bolts or by the H6a and H6b shroud welds.

4. The ring is modeled as a straight bar with an edge crack, under membrane stress equal to the hoop stress of the ring.

5. Limit load analysis of the 304 stainless steel (S_m=16,950 psi) is done to determine the crack/ligament depth at which the ligament stress reaches the $3S_m$ flow stress, also considering a safety factor consistent with ASME Section XI, Appendix C.

6. IGSCC growth is taken at the industry-accepted bounding rate of 5×10^{-5} in/hr, which is conservative considering the moderate hydrogen water chemistry (HWC) levels which are implemented on Unit 1. The low corrosion potentials associated with these HWC conditions would significantly slow, if not halt, IGSCC at the location of the indication.

Analysis

The applied delta-P loads are 34 psi for Normal Conditions (105% rated core flow) and 53 psi for Faulted Conditions (105% rated core flow). With the Section XI safety factors of 2.77 and 1.39 for normal/upset and emergency/faulted conditions, respectively, the normal operation load and safety factor are bounding. The conservative loading assumption yields a normal operating stress in the ring of 2 ksi.

With a flow stress of $3S_m$/SF, the limit load ligament stress is 18.4 ksi. The allowable ligament is therefore (2 ksi * 4 inch) / 18.4 ksi = 0.4 inches. Therefore, the allowable flaw length is 3.6 inches across the entire 6.5 inch depth of the ring.

Allowing for the bounding IGSCC rate over an 18 month fuel cycle, the indication could grow 0.6 inches in one cycle of operation, to 0.9 inches. This is considerably smaller than the 3.6 inch allowable flaw length, so ring integrity is assured for at least one operating cycle.

Other Considerations

1. The shroud ring supporting the core plate is part of the load path which maintains tension in the shroud repair tie rods. Cracking which might degrade the ring stiffness is not a concern because the shroud shells above and below the ring are not offset. The ring material between the shells provides the same compressed material for the load path whether the ring is cracked or not. Therefore, ring cracking as described here does not degrade the shroud repair function.

2. Shroud ring cracking may provide a leakage path for higher pressure water inside the shroud. Such leakage, if any, would be insignificant when compared to the flow through the core during normal operation or the injection into the core by ECCS systems. There would be no significant impact on operation or on design basis accident scenarios.

3. There are six segment welds in the ring. The indication reported here was at the 180° segment weld. The 0° segment weld was also inspected and had no indications. The other four welds are inaccessible for visual inspection. Cracking, if any, in the other segment welds should not be much different from that in the 180° weld. The results of this evaluation apply to cracking in all six segment welds.

Conclusions and Recommendations

This analysis conservatively envelopes the results which would be obtained by a more rigorous analysis, analytically proves that the indication is well within allowable limits, and can be used as the basis for a determination that the ring segment is acceptable as-is without any further action at this time.

It is recommended that the indication be reinspected in accordance with the guidelines of BWRVIP-07.

Supporting calculations and evidence of verification are contained in design record file B13-01869-122. If you have any questions, please call me at the number below.

Regards,

Tom Caine

Verified: H S Mehta

TA Caine, Manager
Structural Mechanics and Materials
(408) 925-4047

HS Mehta, Technical Leader
Structural Mechanics and Materials

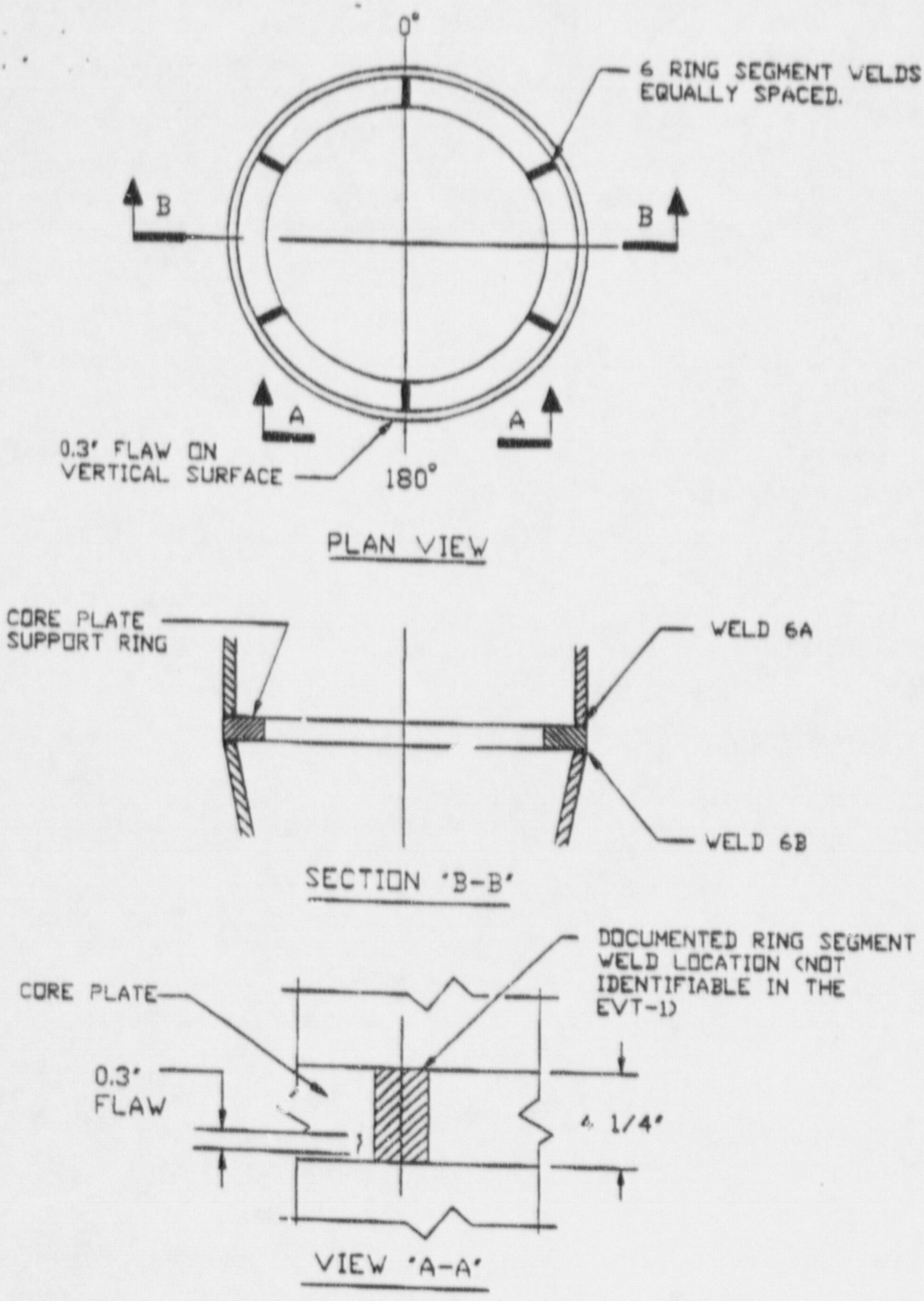

Figure 1. Location of Indication